



INSTITUT DE FRANCE
Académie des sciences

Comptes Rendus

Chimie

Jean-Pierre Cuif, Kadda Medjoubi, Andrea Somogyi, Yannicke Dauphin and Dominique Bazin

From visible light to X-ray microscopy: major steps in the evolution of developmental models for calcification of invertebrate skeletons


Volume 25, Special Issue S1 (2022), p. 577-595

Published online: 6 October 2021

<https://doi.org/10.5802/crchim.125>

Part of Special Issue: Microcrystalline pathologies: Clinical issues and nanochemistry

Guest editors: Dominique Bazin (Université Paris-Saclay, CNRS, ICP, France), Michel Daudon, Vincent Frochot, Emmanuel Letavernier and Jean-Philippe Haymann (Sorbonne Université, INSERM, AP-HP, Hôpital Tenon, France)

 This article is licensed under the
CREATIVE COMMONS ATTRIBUTION 4.0 INTERNATIONAL LICENSE.
<http://creativecommons.org/licenses/by/4.0/>



Les Comptes Rendus. Chimie sont membres du
Centre Mersenne pour l'édition scientifique ouverte
www.centre-mersenne.org
e-ISSN : 1878-1543



Microcrystalline pathologies: Clinical issues and nanochemistry / *Pathologies microcristallines : questions cliniques et nanochimie*

From visible light to X-ray microscopy: major steps in the evolution of developmental models for calcification of invertebrate skeletons

Jean-Pierre Cuif^{®*}, ^a, Kadda Medjoubi[®], ^b, Andrea Somogyi[®], ^b, Yannicke Dauphin[®], ^c and Dominique Bazin[®], ^d

^a CR2P Centre de Recherche sur la Paléodiversité et les Paléoenvironnements, UMR 7207, Muséum National d'Histoire Naturelle CNRS Sorbonne-Université, 75005 Paris, France

^b Nanoscopium Beamline, Synchrotron Soleil, 91190 Saint Aubin, France

^c ISYEB Institut de Systématique, Evolution, Biodiversité, UMR 7205 CNRS Sorbonne-Université EPHE Muséum National d'Histoire Naturelle, 75005 Paris, France

^d Université Paris-Saclay, CNRS, Institut de Chimie Physique, 91405 Orsay cedex, France

E-mails: jean-pierre.cuif@orange.fr (J.-P. Cuif),
kadda.medjoubi@synchrotron-soleil.fr (K. Medjoubi),
andrea.somogyi@synchrotron-soleil.fr (A. Somogyi), yannicke.dauphin@upmc.fr
(Y. Dauphin), dominique.bazin@universite-paris-saclay.fr (D. Bazin)

Abstract. The calcareous skeletons built by invertebrate organisms share a paradoxical property. Although growing outside the mineralizing cell layers the crystal-like skeleton units exhibit morphologies and three-dimensional arrangements that imply an efficient link between crystallization process and taxonomy. Almost two centuries of investigation led to a series of developmental models in which biological and physical or chemical influences are variously balanced. Recent innovative methods allow for their re-examination. From control of the overall shape of the shell to photo-spectroscopic evidence at the atomic level, influence of the biological processes on mineral properties may be a widely shared specificity of the calcareous biomineralization mechanism.

Keywords. Calcareous skeletons, Biomineralization models, Hierarchical structures, Biological control, Microscopy.

Published online: 6 October 2021

* Corresponding author.

1. The paradox of calcareous biominerals

In the study of the widely distributed calcareous shells (mostly produced by marine organisms) a major breakthrough occurred in the middle of the 19th century. At that time, the main lines of the zoological classification in which morphology of the calcareous skeletons play a major role were already established. A first synthesis had been produced by Linné [1] and value of shell morphology as taxonomic criteria was also made obvious through development of palaeontological research in the earliest decades of the 19th century. Investigating tertiary fauna from the Paris basin, Lamarck [2], for instance, created many invertebrate genera (mostly molluscs and corals) whose representatives were later found alive in the tropical seas. This point was important at the beginning of geological investigations because the ratio between still living and exclusively fossil genera was the key point to separate the periods in Cenozoic era. When progress of the microscopes and development of appropriate preparative methods allowed for observation of thin sections of these calcareous shells, a wealth of additional information became available. The origin of this innovative step is well known and provides a remarkable example of unexpected results and correlated interrogations.

The Microscopical Society of London (founded 1839) was dedicated to the study of cellular organization of living organisms, a theory whose universality had just been suggested [3,4]. Among the seventeen founders of the Society, the figure of Bowerbank is of particular interest because he focused his investigation on the shells and other biological mineralized structures. In his first results (published in the first issue of the Transactions of the Microscopical Society [5]), followed by more extended works by Carpenter [6,7], conclusion was that, in contrast to the other organs of the molluscs, their shells were not made of cells. This key point was extended to any calcified structure built by invertebrates. Even for unicellular organisms (e.g., Foraminifera or the Haptophyte algae Coccoliths), formation and growth of the mineral units occur in specific spaces inside the cell, but carefully isolated from the biologically active compartment.

Not only are the calcareous structures of the invertebrates *non-cellular*, but between cross-nicols

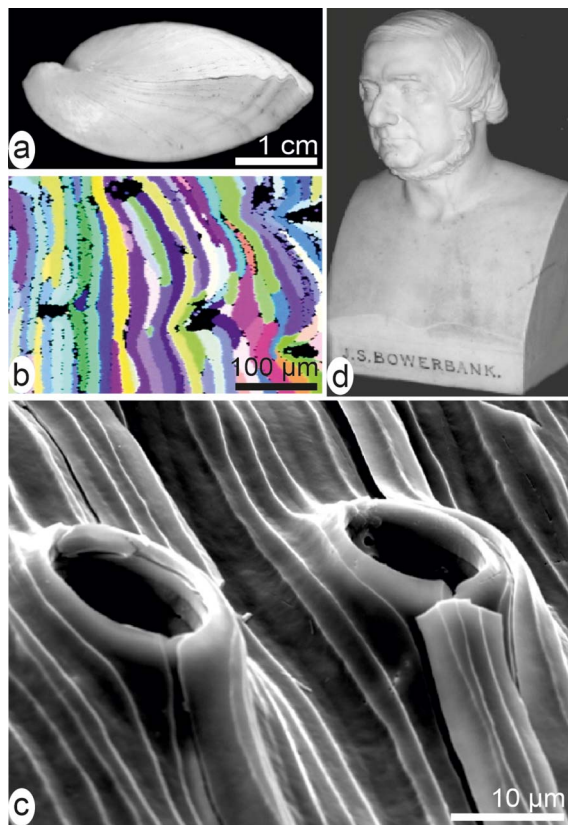


Figure 1. Species-specific morphology of the shell-building units exemplified by fibres in a brachiopod shell (a). Each fibre is a continuous single crystal of calcite ((b) EBSD diagram) whose shape has been adapted to animal anatomy during growth (c) without changing its individual crystallographic orientation. (d) Bowerbank bust.

the mineralized units exhibit crystalline appearances regardless of their shapes (Figure 1a–c). Conclusively, specialized cell layers (e.g., the outer epithelium of the mollusc mantles) produce the chemical components, but crystallization of the shell-building units always occurs outside the mineralizing cell layers, following a process that Huxley assimilated to a secretion [8]. Almost two hundred years later, the mechanism enabling a given species to keep so precise control over construction of its shell that microscopic observation allows for its taxonomic identification remains an unsolved enigma.

From an applied viewpoint, however, the Bowerbank and Carpenter's results were immediately appreciated in another then rapidly evolving research area: the geology of sedimentary rocks, in which the fossilized shells could be now more precisely identified by studying small fragments. Therefore, at Burlington Hall (home of the Geological Society of London) the Bowerbank bust (among very few others) is an expression of the durable impact of his innovative approach (Figure 1d).

Eighty years later, the Schmidt's exhaustive synthesis of microscopic organization of the mineralized structures among living organisms [9] may be considered as an achievement of the Bowerbank and Carpenter's investigations [5–7]. In this milestone study the major patterns and respective importance of the three main types of biogenic mineralized categories were precisely described. Calcium carbonate is by far the most used [10]. It is distributed among most of invertebrate phyla and, accordingly, a remarkable diversity of taxonomy-linked crystal-like building units is generated. Their shapes always differ from the typical forms of the non-biogenic calcite and aragonite. In most cases, a given species can produce two distinct microstructural types simultaneously, with sometimes mineralogical change between the two distinct areas of the mantle as shown by this bivalve (Figure 2a–e).

To emphasize specificity of the calcareous biocrystallization, mention must be made of silica as the second biomineral from a quantitative point of view. Its geological importance was recognized since the beginning of scientific oceanography. First data were collected during Ross explorations of the Antarctic oceans (1839 to 1842) and popularized by the spectacular drawings made by Haeckel [11]. In contrast to Ca-carbonates of the shells, silica is always deposited as amorphous material. However, deposition of this silica is precisely controlled (Figure 3a–d) assessing for the presence of an extremely effective biological process that allows for creation of a precise morphology-based classification for thousands of species.

A third of the major chemical types of biominerals (although of lesser quantitative importance), calcium phosphate, is used in the vertebrate phylum, but also contribute to shell formation in some brachiopods and crustacea [9,12]. Bones (of mesodermal origin) and teeth (mesodermal by the dentine

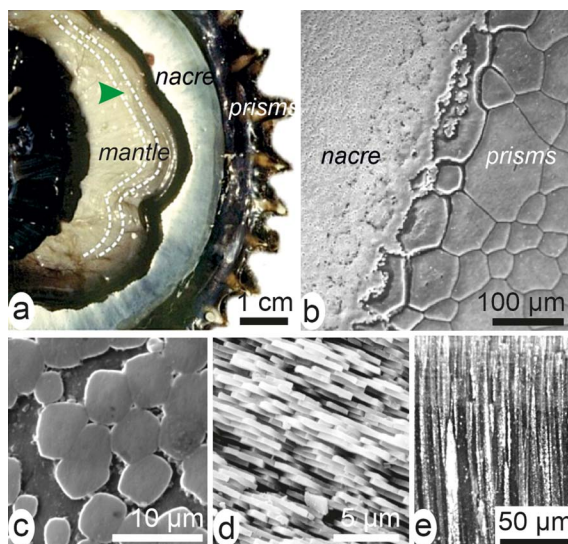


Figure 2. Shell of *Pinctada margaritifera*, the Polynesian pearl oyster. (a) On the inner side of the valve, the mantle is visible but the physical link between the mantle and the shell growing edge has been disrupted. The mantle produces calcite prisms at its periphery (black area of the mantle and shell). The internal light reflective area is the nacre. (b) Enlarged view (SEM) of the contact between prism and nacre areas. (c, d) Nacre built by thin densely packed aragonite tablets parallel to shell surface: (c) front view, (d) lateral view. (e) Prisms are large calcitic polygonal units perpendicular to the internal surface of the shell.

and ectodermal by their enamel) are crystallized materials characterized by the very small sizes of the mineral units (Figure 3e, f) [13]. It is worthwhile to note that when a vertebrate produces calcareous structures (e.g., fish otoliths or eggshells), the mineralization mode closely resembles the invertebrate microstructural growth patterns [10].

In the third decade of the last century, association of biochemical compounds to the mineral phases in the biogenic mineral structures was recognized (or at least hypothesized) in the three major biomineralization mechanisms. Nevertheless, even in the calcareous units whose sizes make observation easily accessible, obtaining precise data regarding relationships between the organic components and the mineral phases was subject to the oc-

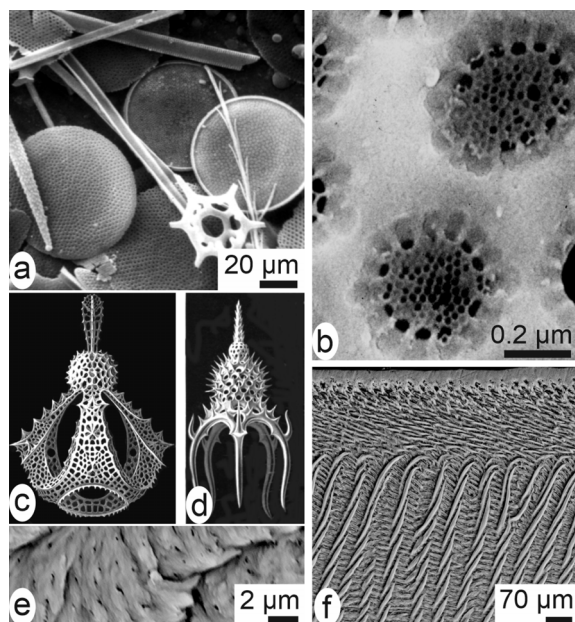


Figure 3. Siliceous and phosphate structures. (a) Diatoms, sponge spicules and silicoflagellid skeletons are typical siliceous materials in the world ocean. (b) Each of the about 1 μm wide holes in a diatom skeleton contains a delicate siliceous grid very precisely controlled. (c, d) Radiolaria drawings by Haeckel [11]. (e) Bone phosphate crystalline units are not visible at the enlargement of the optical microscope. (f) SEM view showing the complex arrangement of enamel microstructure of a rodent incisor, but not the very small crystallite units.

currence of innovative observational and analytical methods. Synchronous with the publication of the Schmidt's synthesis, the famous de Broglie's paper paved the way to electron microscopy [14], but complexity of the calcareous structures and associated biochemical compounds were still far from being deciphered.

2. Attempts to reconcile the crystal-like patterns and taxonomy-linked diversity of the calcareous skeletal units

Once the permanent association between their organic and mineral phases was recognized, the

calcareous biominerals, owing to the frequently large size of their crystal-like units, offer diversified case studies to investigate the respective roles of the two components. The most immediate questionable points were the origin of their obviously controlled crystallographic orientation and in parallel the relationship between this physical pattern and the biological growth mode.

2.1. Biologically induced and matrix-mediated crystallizations

Lowenstam coined these two terms [15] to formally separate the biologically produced calcareous structures depending on the degree of control exerted over their morphology and the three-dimensional arrangements of the mineral units. This distinction appears efficient when comparing the highly organized skeletons produced by the major invertebrate phyla such as molluscs, brachiopods, echinoderms to the disordered arrangement of mineral particles in the green algae, for instance (Figure 4a). Here the small aragonite acicular units are growing without any spatial organization within the organic mucus between the last-order branching structures of the Udoteacea *Halimeda* (Figure 4b–e) or the Dasycladacea.

Position of the coral skeletons exemplifies how uncertain could be the limit between the two branches of the Lowenstam's scheme. Up to 2005, finding statements placing coral skeletons among the weakly controlled structures was possible: “*In “biologically induced” mineralization—for example in corals—the minerals adopt crystal shapes similar to those formed by inorganic processes and have essentially random crystal orientations*” [16]. Actually, such a commonly shared view was based on previous papers emphasizing the similarity of coral skeletal structures with spherulitic crystallization, a chemical precipitation process frequently observed in sedimentary rocks. In corals “*each fibre is a single orthorhombic crystal of aragonite ... we have concluded that these organisms [Hexacoralla] have adopted spherulitic crystallization as an essential mechanism of skeletal development*” [17]. In addition the Barnes's statement that “*three-dimensional arrangement of fibres is due to “crystal growth competition”*” [18] largely contributes to the

interpretation of coral skeletons as weakly controlled materials.

Multiple structural and biochemical evidences have unambiguously placed corals among the “matrix-mediated” calcifying organisms. Most significant is the layered growth mode of the septa and walls, the existence of two distinct mineralizing areas in the basal epithelium synchronically producing specific microstructures with different isotopic fractionations, and the presence of organically coated nanometre-sized grains in both calcitic and aragonitic skeletons [19–21]. All these patterns show that these diploblastic animals also exert a full biological control on their skeletogenesis, equivalent to those of the triploblastic phyla.

2.2. Control of orientation for the crystal-like units: template model and crystal growth competition

Growth of oriented crystals on the surface of organic polymers has been emphasized by Mann [22] as a possible mechanism generating the specific orientation of the skeletal units in the calcareous biocrystallization process. Recent investigation of shell development in the Polynesian pearl oyster *Pinctada margaritifera* exemplifies template process in the early developmental phase of the prisms. But here, in contrast to the classical scheme of direct growth of the oriented crystals onto the polymer surface, a complex developmental process has to be followed at the growing edge of shell to transfer the structural properties of the initial organic grain to each of the distinct individual prisms (see below Section 3.2).

For molluscs and corals as major case study, the long-dominant view was that crystallization of the skeleton units occurs within dedicated spaces between the mineralizing cellular layer and the calcareous structure, e.g. the sub-ectodermal space between the polyp and the underlying coral skeleton (Figure 5a, b) or the hypothesized extrapallial space in molluscs (Figure 5c, d). These spaces were admittedly filled in by liquids in which secretions of the epithelial cells provide the appropriate organic molecules and mineral ions up to fulfilling conditions for precipitation of the calcareous material [23–26]. Accordingly, the specific shapes

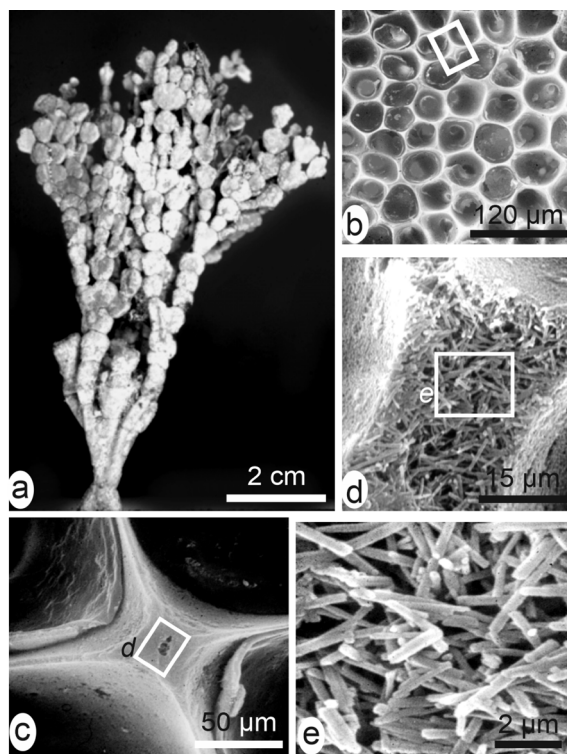


Figure 4. Example of biologically induced mineralization. (a) Dendroid green algae *Halimeda*. (b–e) At the periphery of this algae, disordered aragonite needles crystallize within an organic mucus between the last-order branches.

and three-dimensional arrangements of the skeleton units were considered depending on a “crystal growth competition” process [27,28], based on adequacy between direction of the crystallographic axes and the limited available space between the neighbouring and simultaneously growing units. The diverging fibrous fan systems common in the coral skeletons (Figure 5e) illustrate this apparently competing contact between growing fibres. New preparative methods revealing the micrometric control over growth of these crystal-like units led to modify this purely physical interpretation (Figure 5f, g).

From the classical ionic crystallization mechanism, authors also recognized that taxonomy-linked structural patterns could be due to various additional processes such as development of crystals onto specific organic substrates acting as “template” (e.g., [22]). For instance, when Grégoire and cowork-

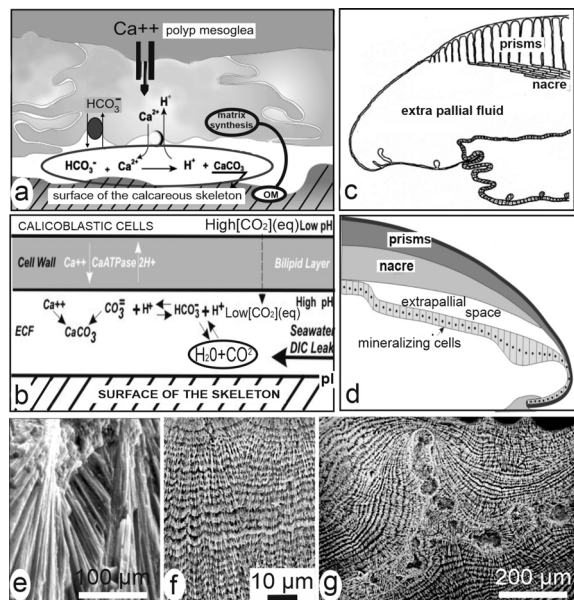


Figure 5. Models of crystallization in liquid-filled chambers. (a) In corals [23], (b) in corals [24], (c) in molluscs [25], (d) in molluscs [26]. (e, f) Biological evidence that growth of coral fibres is not an individual and competitive process but a series of synchronic and biologically controlled mineralization layers. (e) Two neighbouring fibrous fan systems (SEM view of a fractured septa without any preparation). (f) The same area after etching: the two distinct fibrous areas are built by synchronically produced growth layers whose similar thickness variations do not support interpretation by conflictual growth. (g) In the septa of coral skeletons an early mineralization area is built by distinct granular patches later covered by superposed layers of fibrous structures (both aragonite). This double microstructure is a permanent pattern whose three-dimensional variations are linked to taxonomy.

ers carried out a series of investigations about mollusc shells from 1955 to 1977 [29–32], they could observe (using transmission electron microscopy) the alternating organic and mineral layers within the calcareous prismatic structures. The leading role of organic compounds in the formation of the overlying mineral layer was an admitted paradigm.

An alternative mechanism was later suggested in which morphology of the normally growing crystals could be continuously modified by adsorption of species-specific sets of organic molecules onto their lateral faces. This model: “shaping crystals with biomolecules” [33] was followed by emergence of the “non-classical crystallization” theory [34], a collaborative attempt to gather several research areas into a common crystallization mechanism: the “particle attachment” model [35]. The main change is that crystallization is viewed as a two-step process in which tiny initial crystals are admittedly forming larger units by mutual accretion due to interactions between their lateral faces.

Regarding biogenic calcareous structures (also included in this proposed model), the main objection to the hypothesized lateral accretion mechanism was already known: it is that the nanometre-sized building units of the biogenic skeletal units are always lacking crystal faces (see below Section 3.3).

Finally a long series of microstructural observations and chemical measurements have contributed to reduce recognition of the “crystallization chamber model”. It was first disproved by Crenshaw [36] following a biological approach that led him to conclusion that between the mineralizing epithelium and the growing mineral surface “the transfer of material is essentially direct”. The most significant data disproving the existence of a common liquid-filled chamber for crystallization of the skeletal unit were due to occurrence of physical instruments allowing for precisely located measurements of the isotopic fractionation or chemical partitioning. Taking into account the distinct calcareous microstructures, important differences were found *within a given specimen* between the isotopic ratio or trace element concentrations measured in the simultaneously produced minerals of the distinct areas (e.g., [24,37]). As long as measurements were carried out on powders drilled from skeletons without consideration to local microstructure, Urey’s “vital effect” (i.e. the distinct fractionation between species living in the same water pool) was considered as depending on species. As distinct records can be obtained *from a given specimen* depending on the type of skeleton microstructure on which measurements are made, the “vital effect” is not only a matter of species, but is also linked to the distinct biocrystallization processes that may occur within a given specimen.

2.3. A “radical change” in the model of the secretion mechanism for calcareous skeletons: an intracellular phase predating the extracellular crystallization

As crystallization is obviously extracellular, the “direct transfer” process hypothesized by Crenshaw [36] implies that the components secreted by the mineralizing cell layer can directly produce the mineral phase of the growing units. It was about thirty years later that additional information was forthcoming, basically modifying the initial working framework on which previous modelling attempts were relying on.

Intracellular granules found in *Helix* were amorphous Ca carbonate (ACC), and mineralization can occur in vacuoles or vesicles [38]. Then, it was shown that in the growth of a larval spicule of the echinoderms the initially deposited material was made of ACC [39]. Moreover, ACC was shown to be present within cultivated mantle cells of *Pinctada* [40]. Thus, a few years later, to extend these findings to the main calcifying groups, its generalization was considered as a “tantalizing possibility” [41]. In this new view, formation of the calcareous materials involves two distinct phases: the first one produces an accumulation of Ca-carbonate *in amorphous status* within the cells of the mineralizing epithelium. This preparative phase is followed by exocytosis of the amorphous material and its external crystallization.

In elaboration of a developmental model for biogenic calcium carbonate, this two-phased mineralization concept made irrelevant an unsolved key question: the transit through the crystallization chambers of the sea-water volume needed to continuously produce a compact calcareous structure taking into account the low calcium concentration of sea water. This had sometimes led authors to hypothesize some ionic “leaks” that had no anatomical support [24] (Figure 5b). Now the origin of mineral components, far from elucidated yet, is attributed to internal physiological processes [42,43].

In contrast, a very positive result of this “two-phase” calcification model was that an understandable link was made possible with previous approaches developed since the late 70’s, investigations that have made obvious the existence of a layered growth mode of the skeletal units in a wide diversity of calcareous skeletons.

3. Evidence of a generalized layered growth mode for the calcareous crystal-like units and their common granular ultrastructure at the nanometre range

Presence of an organic phase whose distribution was inaccessible to optical observation or X-ray diffraction method led H. Mutvei to develop an etching approach to display the internal structure of the calcareous biominerals. By carefully dissolving the outer organic film surrounding the tablets of nacre (using oxidative–fixative solutions) the respective distributions of organic and mineral phases become visible up to certain extent. Taking advantage of scanning electron microscopy it was thus possible to reveal the internal organization and growth mode even for the few micrometre-sized aragonite of the nacre, usually described as a uniform “brick and mortar” assemblage (Figure 6a, b). This approach deeply modified the common view about the nacre tablets by showing their taxonomy-linked internal diversity [44–47]. Similarly, the inner nano structure of the calcite laths of the foliated layer of oysters was revealed by enzymatic or bacterial etchings [48] (Figure 6c–f).

Applying this method to a wide diversity of calcareous biostructures [49] and focusing attention to the anatomical areas where development of the skeleton units was starting resulted in conceptual change by revealing the unsuspected architectural organization of some reference materials.

3.1. *The Pinna prism internal substructures reveal a three-dimensional stepping growth mode of the shell*

Since the beginning of biomineralization studies, *Pinna* prisms are the reference owing to their geometrical simplicity and perfect calcite crystal-like behaviour (Figure 7a–c). However, etching reveals that within the organic envelopes, two cyclic mineralization systems exist, clearly related to the overall growth of the shell.

The first one is parallel to the internal surface of the shell (Figure 7d: *gl*). It shows that the prisms whose elongation is produced by addition of superposed growth layers (Figure 7e) are synchronically growing through a coordinated stepping mode. This synchronic growth mode of the whole prismatic surface is clearly demonstrated by electron microprobe

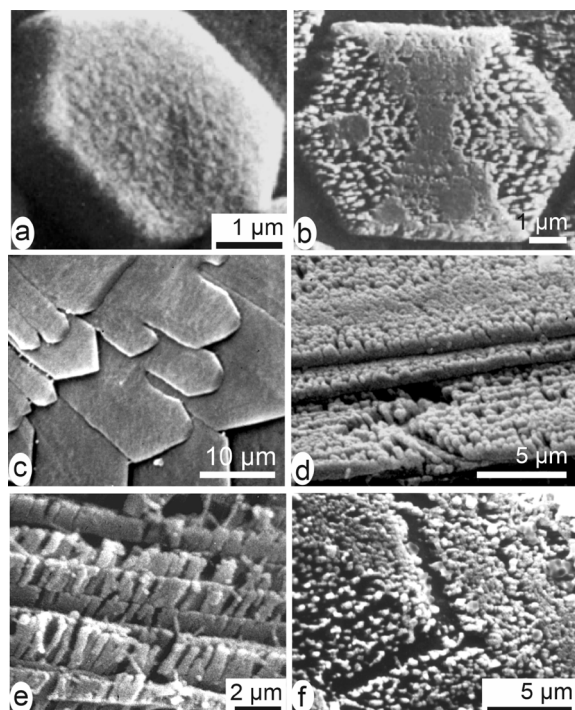


Figure 6. Layered growth mode of calcareous biocrystals. Nacreous tablets of *Unio* before (a) and after (b) etching (from [43]). (c) Foliated microstructure of the internal layer of *Crassostrea gigas* before etching. (d–f) Linear arrangement of the calcified units. Note that (a, b) pictures are from an aragonite biocrystal, pictures (c–f) are from a calcite one.

mapping of the polished surface (Figure 7f, g). This shows that traces of environmental chemical or isotopic variations can be inserted into the shell through the pulsed growth mode of the skeletal units. Each growth layer appears as a crystallization unit whose composition varies from layer to layer [50].

In addition, a second crest-and-groove system is visible on the etched surface: it is slightly oblique with respect to overall geometry of the prisms (Figure 7d: *or*). It is linked to lateral extension of the shell (Figure 8a). In contrast to their apparently distinct geometry (emphasized by crystallography) a remarkable correspondence exists between neighbouring prisms. The second crests-and-groves system is well coordinated (Figure 8b, c) through the organic envelopes surrounding each prism. This shows that the lateral extension of the shell is also a stepping

process [51]. It is obtained by synchronic deposition of elongation layers coordinated between neighbouring prisms a process that is also visible on their lateral faces (Figure 8d).

Applying the “two-phases” mineralization model to the layered structure of the *Pinna* prisms offers an understandable solution to their paradoxical properties. For each growth layer, deposition of amorphous material is followed by crystallization driven by the previously crystallized substrate (i.e. the internal surfaces of the prisms that play a template role). As a result, individual crystallographic patterns are maintained from a common amorphous mineral deposition. So, the outer shell layer of *Pinna* is not a simple juxtaposition of independent crystal-like units as suggested by polarization microscopy. It is a wholly integrated three-dimensional structure in which the stepping secretion process of the mantle simultaneously increases thickness and lateral dimensions.

3.2. Prisms from their early beginning: origin of the distinct crystallographic orientations in the prisms of *Pinctada margaritifera*

In contrast to investigations that deal with well-established prisms, the microstructural approach applied to the growing edge of the shells provides information about the complex ontogenetic process that drives their initial stages.

A fully open shell (e.g., Figure 2a) displays a wrong picture of the relationships between mantle and shell. In the natural status of any pelecypod mollusc a physical continuity exists between the animal and its shell valves: this continuity is ensured by the periostracum [52–54]. This is an organic membrane secreted by a specialized group of cells located in the outer mantle groove (Figure 9a). In *Pinctada* it directly contributes to shell formation [55,56] because it acts as a conveyor belt and transports on its internal side the earliest calcified materials of the shell.

The mineralizing cells of the mantle groove produce organic grains deposited onto the internal side of the periostracal membrane (Figure 9a, b: arrows). Calcification occurs around these initial mineralization centres (Figure 9b–d) following a concentric stepping process (Figure 9e). These disks have a crystal-like behaviour, each of them with slightly distinct orientation [57]. Thus, numerous flat disks

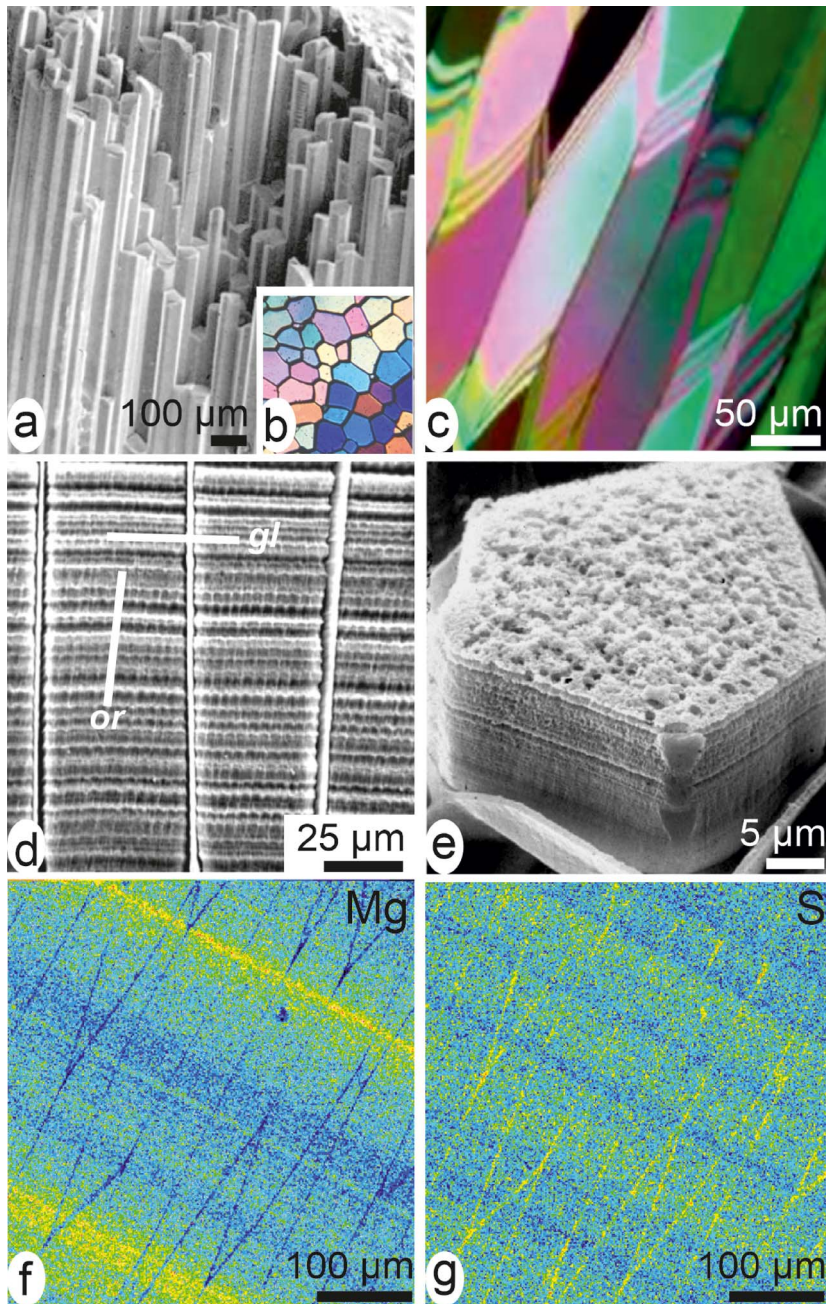


Figure 7. From crystal-like to layered structure of a *Pinna* calcite simple prism. Rectilinear polygonal prisms (a) appear as single crystal units in both transversal (b) and slightly oblique longitudinal (c) sections between cross-nicols. (d) Etched longitudinal sections reveal the superposed growth layers synchronic through the whole mineralizing surface of the shell (*gl* = growth lines) and the series of shell elongation units (*or*) (see also Figure 8). (e) Sides of a young prism show its layered growth mode; note the “non-ionic” growth pattern of the upper surface. (f, g) Distribution of sulphur and magnesium emphasizes the layered growth mode and the distinct absorption of chemical elements within each superposed layer: each growth layer is an independent crystallization unit.

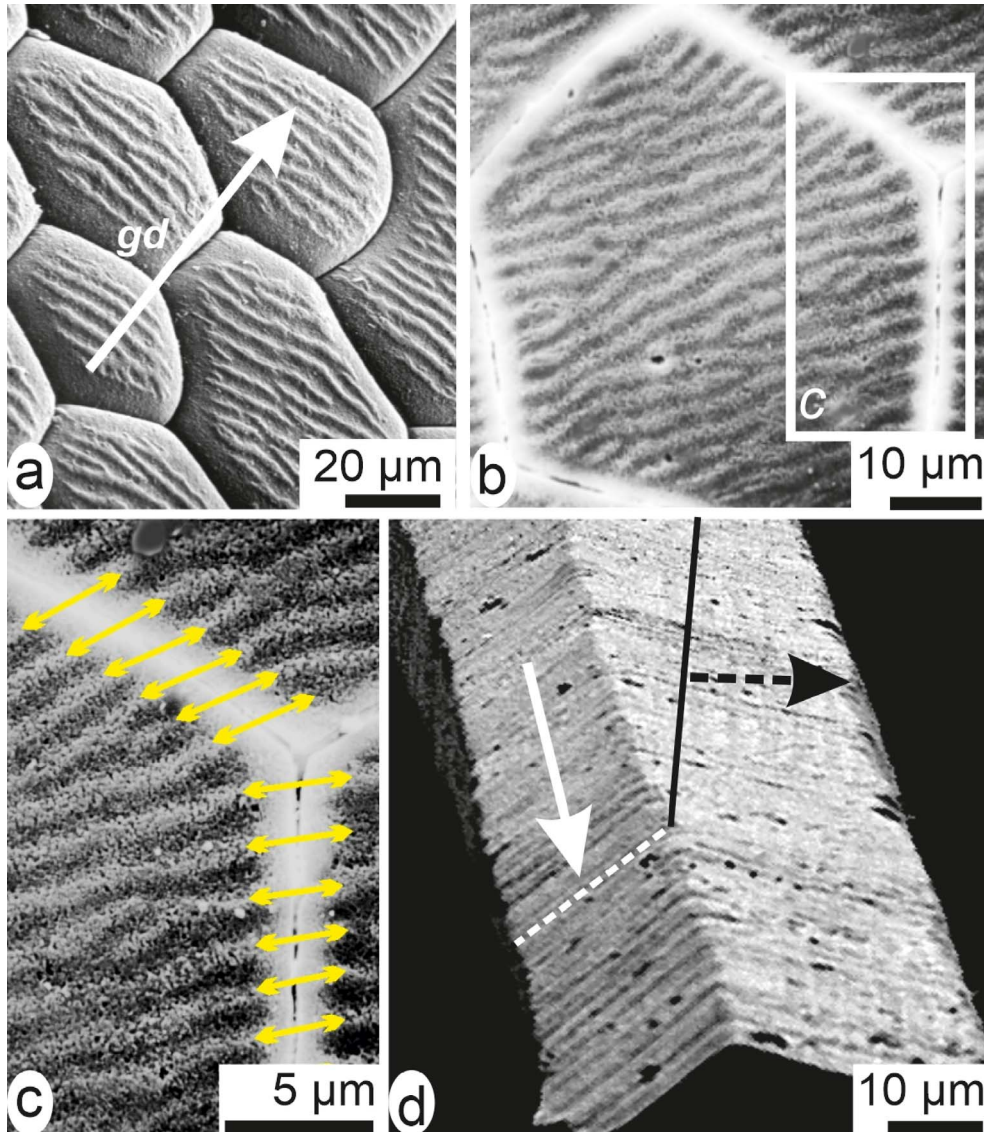


Figure 8. Two-dimensional stepping growth mode of the *Pinna* prisms. (a) On the actively growing internal surface of the *Pinna* shell a crest-and-groove system is visible, perpendicular to growth direction of the shell (*gd* arrow). (b, c) SEM view of a polished surface in the same area: note the correspondence of the lateral growth layers between neighbouring prisms, showing that elongation of the whole shell is a coordinated process. (d) Lateral faces of an isolated prism showing traces of the stepping elongation: orientation of the traces depends on orientation of the prism faces with respect to growth direction of the shell.

are formed with thickness never exceeding 3–4 μm with diameter reaching 20–25 μm . This is the “flexible shell”, in which disks are growing independently as crystallographically distinct units [57–59].

Reaching the growing edge of the shell, the periostracal disks are used as substrates for prism

formation (Figure 9f). As in the *Pinna* shell (Figure 7b) prisms of the *Pinctada* are distinctly oriented as shown by polarized light (Figure 9g) in spite of the synchronic production of the growth layers. Secretion of the shell growth layers as amorphous material explains the distinct crystallization

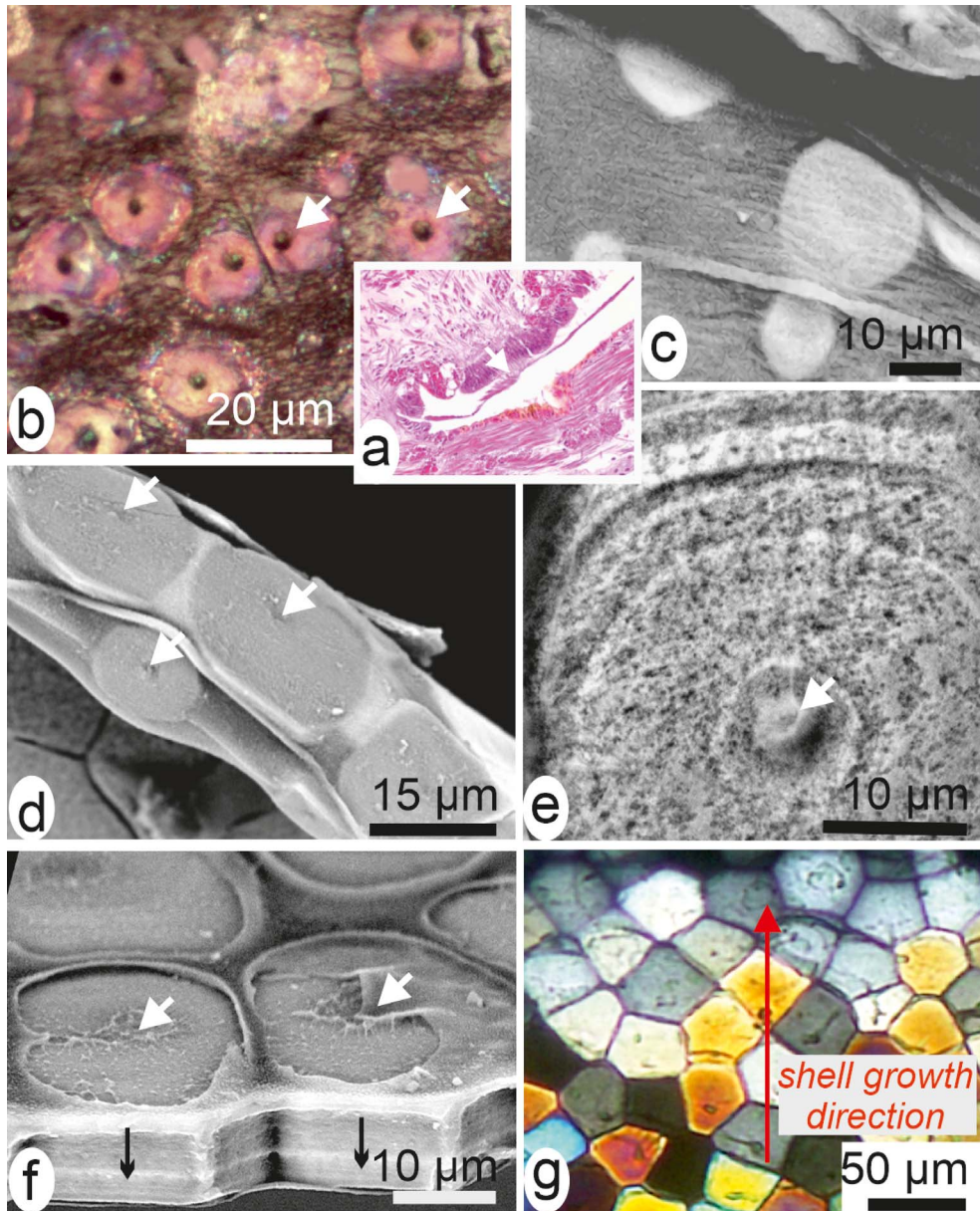


Figure 9. Example of a double transfer of substrate orientation in the development of the prisms in *Pinctada margaritifera*. (a, b) Close to the formation of the periostracum in the outer mantle groove small patches of organic material are deposited on its internal surface (arrows). (c–e) Repeated concentric depositions of calcite results in formation of flat disks. (f, g) At the shell growth edge, disks are shown forming the top of the prisms; (f) distinct crystallographic orientations of the prisms is visible between cross-nicals; (g) emphasizing the initial differences between the initial disks.

of the prisms. The amorphous layer synchronically secreted by the mantle crystallizes according to crystallographic orientation of the disk it is facing. Polarization colours passing from first-order

grey to the end of first order (Figure 9g) show that once established the initial crystallographic differences between neighbouring prisms are maintained [57–59].

Therefore early development of the *Pinna* and *Pinctada* prism layers exemplifies how the concept of “template model” must be carefully examined, taking into account the series of ontogenic events that occurs not only at the shell growing edge but also in the deeper part of the outer mantle groove. A first template process occurs when crystallization of the periostracal disks is based on the organic grains secreted onto the internal side of the periostracum, a second one occurs when the resulting disks provide support to the early stages of disk growth.

In conclusion, these two admittedly “simple” prisms revealing distinct development processes, but in both cases the two-phase mineralization mechanism contributes to explain their respective specificity.

3.3. The common granular ultrastructure of the calcareous units observed at the nanometre scales

In parallel to evidence that the calcareous shell-building units may exhibit distinct internal architectures a surprising similarity of their structural pattern at the nanometre range was made obvious by using atomic force microscopy (AFM).

Owing to its capability to simultaneously capture distinct signals corresponding to different material properties, this method provides us with information about organization of the calcareous biominerals with an unprecedented resolution. It has shown that calcareous growth layers were built by round-shaped nanometre-sized mineral grains (Figure 10a–f) surrounded by organic material. The densely packed spheroidal grains are illustrated by Figures 10a, b and 10c, d, in aragonite of cephalopod nacre [60], coral fibre [61] and brachiopod fibre (calcite) [62]. They have been observed in materials biologically distant like fish otoliths [63], eggshells [64], calcareous sponges, foraminifera, etc. Everywhere the typical AFM phase-contrast imaging indicates the presence of a highly interactive phase (strongly adherent to the AFM cantilever tip) at the periphery of the grains (Figure 10e, f).

In the concept of an intracellular preparative phase predating exocytosis, crystallization of ACC within the mineralizing cells must be prevented by organic compounds [65]. After exocytosis, crystallization occurs and reticular structures are now visible

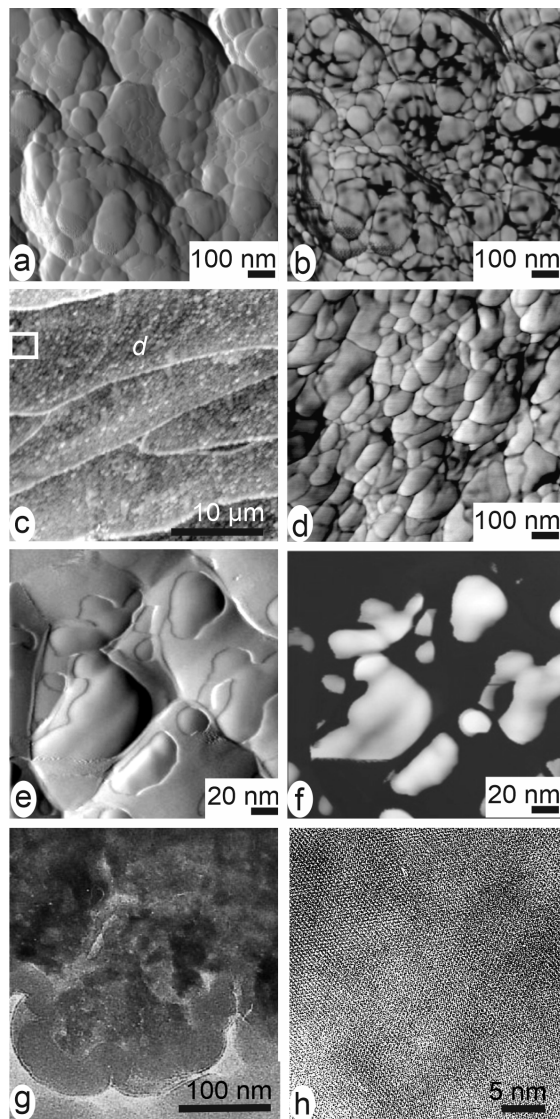


Figure 10. Coated-mineral grains common to biogenic calcareous structures. Independently of the producing phylum, the layered growth units in calcareous structures are built by infra-micrometre-sized grains (in the range of the 50–150 nanometres). (a, b) Coral fibres. (c, d) Brachiopod fibres. (e, f) *Pinctada margaritifera*, amplitude (e) and phase-contrast (f) images of the calcareous grains showing the correspondence between the peripheral envelopes (e) and their strong interaction with the AFM tip (f). (g, h) Transmitted electron images of the grains: below the organic coating, grains are well crystallized.

in the nanometre-sized units (Figure 10g, h). The organic compounds that have prevented amorphous crystallization inside the cells are now squeezed between the crystallizing grains preventing formation of faceted surfaces.

That similar nanometre-sized spheroidal structure was found in every calcareous biocrystal, whatever their taxonomic origin, indicates that an equivalent process is running in every calcareous biomineralization [66]. From an evolutionary view point, this remarkable consistency of the infra-micrometric structural organization suggests that any biological system having developed a calcification process was submitted to common requirements linked to basic chemical properties of the Ca-carbonates.

With respect to molecular diversity of the intraskeletal organic materials, the “two-phases” mineralization concept opens a plausible explanation to the biochemical complexity of the organic matrices. Over several decades, attempts to establish a structural relationship between organic and mineral components were almost exclusively based on proteins [67,68], owing to technical improvements that allows for protein sequencing and amino-acid analysis [69]. In contrast, no role was attributed to the polysaccharides although their presence was established and sometimes emphasized specifically in the sulphated form [70–72]. Evidence now emerges that taxonomy-related chemistry involved in the formation of amorphous material during the intracellular phase of the mineralizing process is a prerequisite to understand the crystallization process of the structural units.

4. Abnormal mineralization in pearls: evidence for a recovery process leading to nacre deposition

Among the diversity of the calcareous materials produced in the living world, nacre has long attracted attention. Built by densely packed flat aragonite tablets (Figure 2c, d), nacre reflects visible light at the tablet surfaces (in contrast to other calcium carbonate structures). This property becomes of particular interest in the mollusc class Pelecypods because, inside their bivalved shells, some families can produce rare round-shaped bodies whose ornamental power has long been noticed: the pearls.

In the first decade of the last century Mise and Nishikawa elaborated the pearl cultivation method which essentially remains unchanged up to now. It involves two “pearl oysters” and comprises a surgical operation. A small fragment of the nacre producing mantle tissue—the “graft”—is first cut from one of these oysters (the “donor”). It is then transported into a “recipient” oyster and deposited onto a spherical body (the “nucleus”) previously introduced into the “pearl pocket” (a part of the pelecypod gonad). Inside this pocket the graft spreads by cellular multiplication up to a complete wrapping of the nucleus, producing the “pearl sac” in which pearl grows during about two years and is then collected.

Over decades it has been admitted that onto the nucleus surface the graft was producing the same nacre as it was doing just before being cut from the animal mantle. Therefore the observation by Kawakami [73,74] that *calcite deposition* may occur during early development of pearls can be considered as a major step in biomineralization studies. It is important from a practical view point (calcite deposition is a major cause of morphological irregularity in pearls); moreover calcite deposition reveals in-depth alteration of the well-established process that was running in the graft cells when it was a part of the mantle. Comparison between Figure 2c, d (*Pinctada* nacre) and Figures 11–12 (early pearl mineralization) reveals how important perturbation of the mineralizing process can be. Therefore, exploring the early stages of pearl formation was a thoroughly investigated topic in Japan during the second half of the last century [75–77]. More recently deposition of calcite was integrated in a general concept of the pearls viewed as a “reversed sequence of layers” of the shell [78].

Investigations using standard X-ray characterization and XANES mapping have shown that the reversed shell hypothesis does not account for the sequence of structural events that can be observed during early stages of pearl formation [79]. Recent developments in X-ray microscopy [80] provided high-resolution evidence suggesting that the long and somewhat erratic recovery pathway by which nacreous secretion is finally restored in the cultivated pearls could be informative about the control of the biomineralization process [81,82].

In place of nacre the mineralized units produced by the newly formed pearl sac frequently appear as

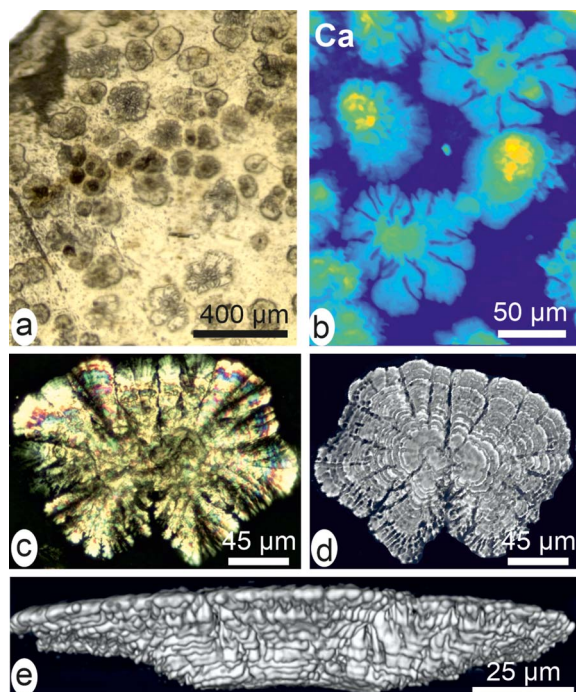


Figure 11. Early mineral deposition after a 20-day post-grafting cultivation (compare to nacre in Figure 2c, d). (a) Distinct patches in a detached fragment. (b) High-resolution X-ray fluorescence showing the radial expansion of the mineralization. (c) Radiating unit between cross-nicols. (d) Full field tomography showing the inferior face of the unit. (e) Reconstructed lateral view showing its mode of growth by superposed layers with increasing diameters.

distinct patches ranging in size from 50–100 μm (Figure 11a, b). Their irregularly radiating growth is well evidenced by high-resolution X-ray Ca fluorescence. Polarization shows their radiating crystallization (Figure 11c) but phase-contrast imaging reveals their layered structure. Figure 11d (lower surface of the unit) and Figure 11e (lateral view) show that these units are not simple mineral spherulites. They are built by repeated superposition of micrometre-thick calcified layers whose diameters are regularly increasing. This shows that in spite of the strong degradation of the mineralizing process the fundamental layered growth mode has been preserved in the pearl sac.

A 30-day post-grafting sample illustrates important changes in mineralization as the early stages

are now covered by continuously mineralized surfaces (Figure 12a–c). Previous investigations using standard X-ray diffraction had shown that components of the neighbouring areas were heterogeneous with respect to mineralogy [81,82]. High-Resolution X-ray fluorescence mapping allows for fine scale microstructural patterns and elemental distribution (Figure 12d–g).

It is important to emphasize that, in contrast to the regularity of the mineralization in shells, these early developmental stages of the pearls reveal a high structural and compositional diversity. As the grafting process requires time consuming operations, it may generate various levels of disturbance in gene expressions in the pearl-sac cells. Abnormal structures made of calcite and non-nacreous aragonite exemplify such perturbations as they can be simultaneously produced, each of them with different organic contents (Figure 13a–d) and [79, Figures 4–5], [82]. Remarkably, recovery of the nacre production process generally occurs after times varying from days to weeks and sometimes months. Structural examination of the transitional areas (Figure 13a–d) and variation in the corresponding XANES maps (Figure 13e, f) show that in the superposed growth layers the boundary between abnormal mineralization and true nacre secretion is not straightforward. In the Polynesian pearls a progressive return to nacre is made visible by the spreading of the black pigment (Figure 13b). From a biochemical view point replacement of calcite by nacre is correlated to the end of polysaccharide secretion (Figure 13e).

From an overall viewpoint, what appears more significant is the surprising ability of the pearl sac to reproduce nacre deposition through various transitional pathways. This makes it obvious that some biological control over pearl-sac secretion related to initial production of nacre by the graft has persisted through the abnormal mineralization period.

5. Conclusion: converging evidences of a multi-scale biological control over developmental process in the matrix-mediated biomineralizations

Investigations dealing with pearls provided evidence of a multiscaled biological control over developmental process in the matrix-mediated biomineralizations.

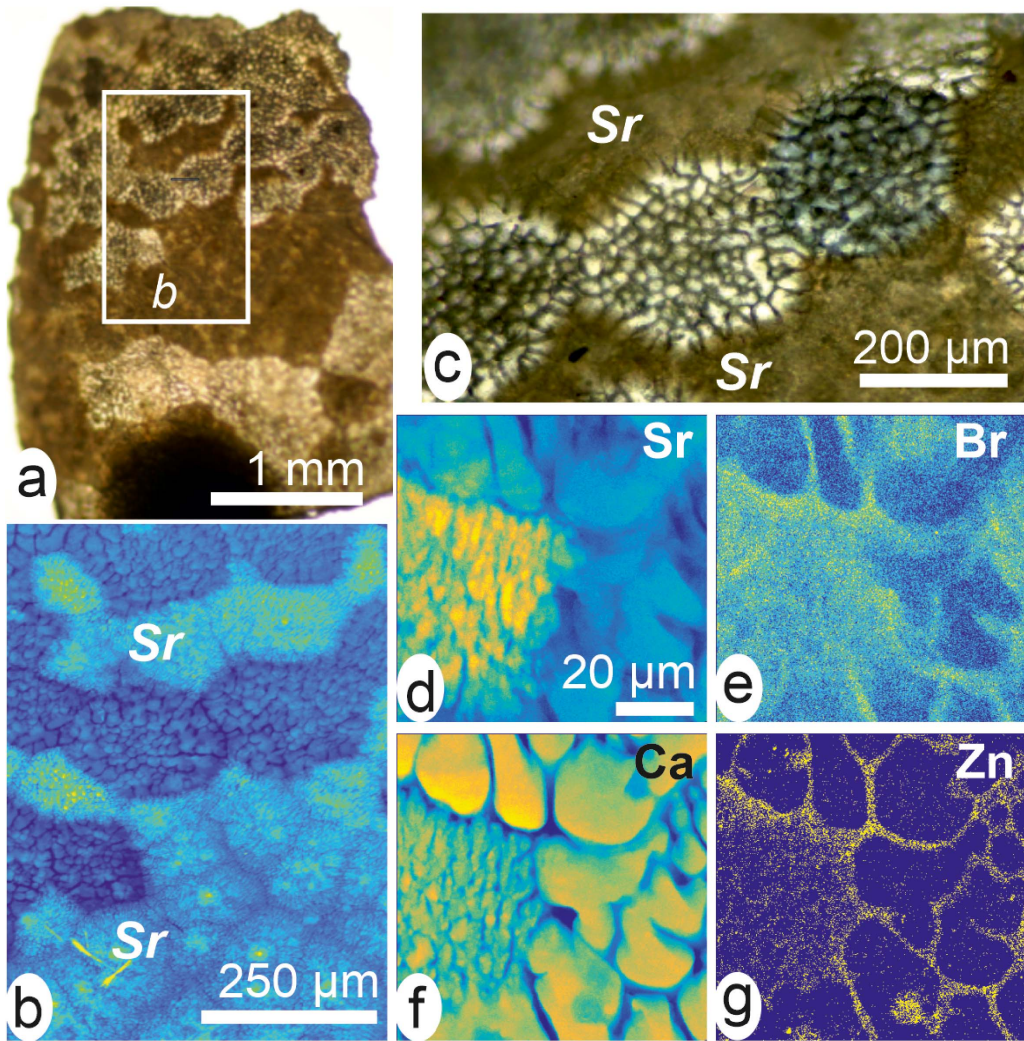


Figure 12. High-resolution X-ray fluorescence maps of the early mineralization stage in a cultivated pearl of *Pinctada margaritifera*. (a, b) Optical views of a fragment showing distinct mineralization patterns. (b) Between Sr-rich areas, crystallization occurs by forming distinct grains consistently polarizing within polygonal areas. (e–g) Distribution maps of Sr (d), Br (e), Ca (f) and Zn (g) in the same fragment. Note the clearly distinct morphologies of the mineral units between high and low Sr contents areas.

Nowhere are the relationships between biology and crystallization more apparent than in this several decade-old figure by Wada [76] in which a close correspondence is shown between crystallographic orientations of the nacreous tablets and growth directions in the shell of *Pinctada martensi* (Figure 14a, b). This obviously implies that nucleation and growth of the tablets are related to an oriented organic framework whose directional changes during ontogeny in-

duce correlative modifications in orientation of the mineral units. Note that overall tablet orientation is not the only biologically influenced feature: crystallization of the nacreous tablets also depends on biological control. In sedimentary aragonite, the main growth direction for aragonite is the *c*-axis, leading sometimes to production of acicular crystals in the *c*-direction. In contrast, in the nacre aragonite tablets the *c*-axis is perpendicular to the flat surface,

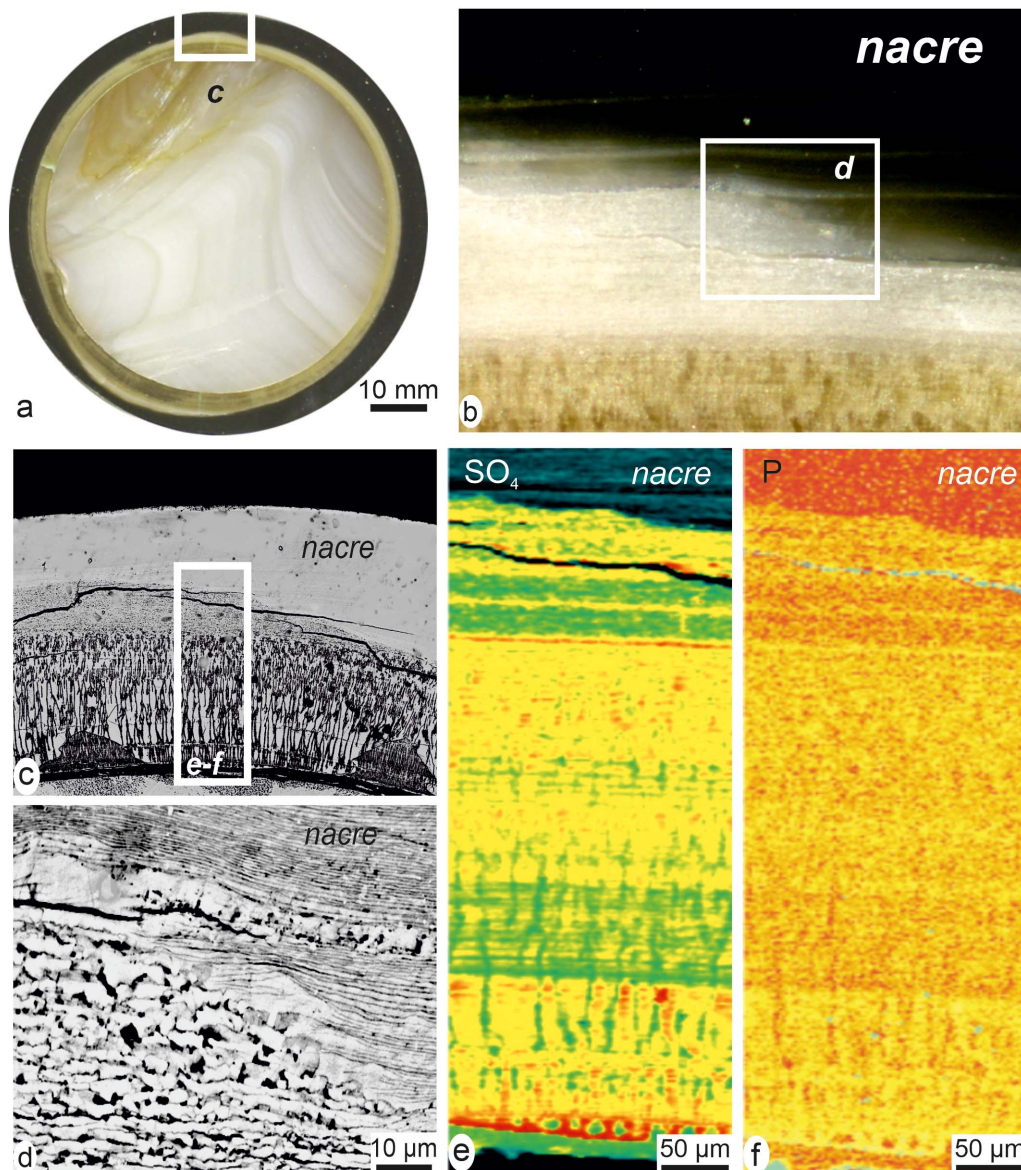


Figure 13. The stepping return to nacre production in cultivated pearls. (a) The external black nacreous layer makes the abnormal mineralization phase well visible. (b) Enlarged view of the extension of the nacre, progressively replacing the complex lower layer. (c) The radial envelopes (perpendicular to nucleus surface) may contain calcite or non-nacreous aragonite. (d) Enlarged view of the contact line between true nacre (note the specific layering) and abnormal mineralization. (e, f) XANES distribution of sulphated polysaccharides (e) and phosphorus (f) during the abnormal mineralization period. Note the progressive metabolic changes in the upper layers of the field, corresponding to nacre expansion.

showing that in this direction growth is restricted at about 1/10 ratio, resulting in the optical property of the nacre [76].

Biological influence on crystal growth is also obvious in the prisms of the *Pinctada* shell. Not only is the *c*-axis perpendicular to the main growth direction

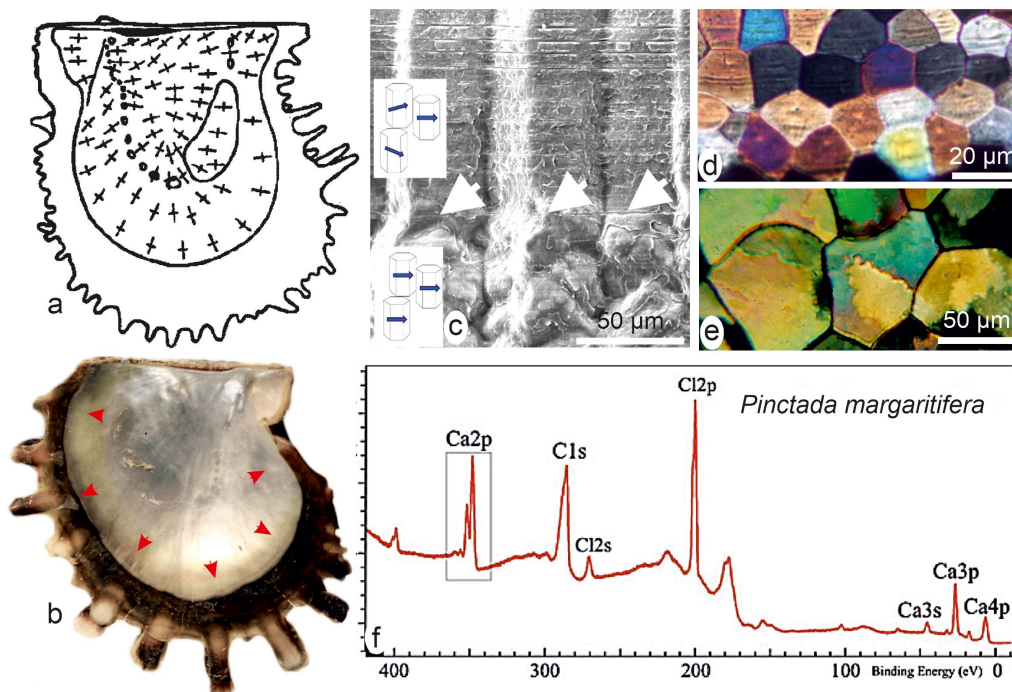


Figure 14. Multi-scaled evidences of organic–mineral interactions during shell formation from overall growth up to atomic level. (a, b) Tablets of nacre have their *a*- and *b*-axes consistently oriented with respect to direction of shell expansion ((a) original figure in [76]). (c–e) Modification of crystallization patterns during growth of the prisms of a *Pinctada* shell. (f) Taxonomy-linked shifted values of the Ca2p binding energies suggest interaction with the species-specific mineralization matrices and origin of abnormal crystalline parameters of the resulting mineral phases [83].

of the prism [84], but a microstructural change regularly occurs in the prisms after about 150 to 200 μm of thickness increase (Figure 14c, arrows) [85,86]. This has unexpected crystallographic consequences (Figure 14g, h). In the initial growth stages (single-crystal like), the *c*-axes are differently oriented whereas in the second growth phase, much more disordered with respect to microstructural arrangement, the *c*-axes are more consistently oriented perpendicular to growth direction [84].

Thus, in the *Pinctada* shell, growth of both calcite and aragonite units demonstrate opposite behaviour with respect to the common views regarding crystal growth. It shows that influence of the biochemical compounds that drive mineralization of the shell-building unit is predominant over admitted rules for chemical crystallization.

Looking at the lowest structural levels, the organic coating of spheroidal nanometre-sized units has suggested that these components may play a

key role in preventing the development of faceted nanocrystals (no particle attachment model). Interestingly, synchrotron-based photo-emission spectroscopy carried out on the soluble part of the organic compounds extracted from calcite or aragonite skeletons have shown that the binding energies of Ca orbitals were significantly distinct from the corresponding values in pure calcite or aragonite (Figure 14f). Distinct values have been observed depending on the taxonomy of the organism from which organic compounds are coming from [83]. This establishes that organic compounds extracted from Ca-carbonate nanograins have preserved their binding capabilities to the calcium atoms. This could be the reason why crystallization of the growth layers results in rounded grains and not the faceted crystals occurring in non-biogenic crystallization [87].

Conclusively, comparative investigations now possible for each of the structural levels allow for

in-depth examination of materials produced by abnormal or pathological mineralization processes in both animal and human biology. Animal mineralization disturbances (such as deficiency in formation of coral skeletons) may result in global consequences at the world-wide oceanic level. Conversely deciphering ultrastructure and growth mode of the abnormally mineralized materials may contribute to the understanding of biological/environmental imbalance in human pathologies.

Acknowledgements

This study was supported in part by SOLEIL Grants 201770784 and 20180995 to J-PC and YD.

References

- [1] C. Linné, *Systema naturæ per regna tria naturæ, secundum classes, ordines, genera, species, cum characteribus, differentiis, synonymis, locis*, Impensis L. Salvii, Holmiæ, 1758.
- [2] J.-B. Lamarck, *Mémoire sur les fossiles des environs de Paris*, Annales du Muséum d'histoire naturelle, 1802–1806, vol. 1–8, Muséum d'histoire naturelle, Paris, 1802.
- [3] M. Schleiden, *Archiv für Anatomie, Physiologie und wissenschaftliche Medicin*, Verlag von Veit et comp., Berlin, 1838.
- [4] T. Schwann, *Mikroskopische Untersuchungen über die Uebereinstimmung in der Struktur und dem Wachstum der Thiere und Pflanzen*, Sander, Berlin, 1839, 268 pages.
- [5] J. S. Bowerbank, *Trans. Microsc. Soc. Lond.*, 1844, **1**, 123–152.
- [6] W. Carpenter, *Br. Assoc. Adv. Sci.*, 1844, **14**, 1–24.
- [7] W. Carpenter, *Br. Assoc. Adv. Sci.*, 1847, **17**, 93–134.
- [8] T. H. Huxley, *Proc. Zool. Soc. Lond.*, 1879, **46**, 751–788.
- [9] W. J. Schmidt, *Die Bausteine des Tierkörpers in Polarisiertem Lichte*, F. Cohen, Bonn, 1924.
- [10] H. Lowenstam, S. Weiner, *On biomineralization*, Oxford University Press, New York, 1989, 324 pages.
- [11] E. Haeckel, *Die Radiolarian (rhizopoda Radiara). Eine Monographie*, Reimer, Berlin, 1862.
- [12] N. Watabe, C. M. Pan, *Am. Zool.*, 1984, **24**, 977–985.
- [13] S. Weiner, W. Traub, *Connect. Tissue Res.*, 1989, **21**, 259–265.
- [14] M. de Broglie, *J. Phys. Radium*, 1924, **5**, 1–19.
- [15] H. A. Lowenstam, *Science*, 1981, **211**, 1126–1131.
- [16] A. Veis, *Science*, 2005, **307**, 1419–1420.
- [17] W. H. Bryan, D. Hill, *Proc. R. Soc. Queensland*, 1941, **52**, 78–91.
- [18] D. J. Barnes, *Science*, 1970, **170**, 1305–1308.
- [19] J. P. Cuif, Y. Dauphin, *Paläont. Zeit.*, 1998, **72**, 257–270.
- [20] J. P. Cuif, Y. Dauphin, *Biogeosciences*, 2005a, **2**, 61–73.
- [21] J. P. Cuif, Y. Dauphin, *J. Struct. Biol.*, 2005b, **150**, 319–331.
- [22] S. Mann, *Biomineralization: Principles and Concepts in Bioinorganic Materials Chemistry*, Oxford University Press, Oxford, 2001.
- [23] P. Furla, I. Galgani, I. Durand, D. Allemand, *J. Exp. Biol.*, 2000, **203**, 3445–3457.
- [24] J. F. Adkins, E. A. Boyle, W. B. Curry, A. Lutringer, *Geochim. Cosmochim. Acta*, 2003, **67**, 1129–1143.
- [25] H. Petit, “Recherches sur des séquences d'événements périostaux lors de l'élaboration de la coquille d'*Amblema plicata* Conrad, 1834”, PhD Thesis, Lab. Zoologie, Université de Bretagne occidentale, France, 1978, Thèse doc. Lab. Zoologie, 276 pages.
- [26] D. Volkmer, “Biologically Inspired Crystallization of Calcium Carbonate beneath Monolayers: A Critical Overview”, in *Handbook of Biomineralization. Biomimetic and Bioinspired Chemistry* (P. Behrens, E. Bauerlein, eds.), Wiley VCH, Weinheim, Germany, 2007, 65–87.
- [27] J. D. Taylor, W. J. Kennedy, A. Hall, *Bull. Br. Mus. Nat. Hist. Zool.*, 1969, **63**, 1–125.
- [28] A. G. Checa, T. Okamoto, J. Ramirez, *Proc. R. Soc. Lond. B*, 2006, **273**, 1329–1337.
- [29] C. Grégoire, G. Duchateau, M. Florin, *Ann. Inst. Océanogr.*, 1955, **31**, 1–36.
- [30] C. Grégoire, *Biol. Rev.*, 1967, **42**, 653–687.
- [31] C. Grégoire, *Bull. Inst. R. Sci. Nat. Belg.*, 1960, **36**, 1–22.
- [32] G. Goffinet, C. Grégoire, M. F. Voss-Foucart, *Arch. Intern. Physiol. Biochem.*, 1977, **85**, 849–863.
- [33] J. J. De Yoreo, P. M. Dove, *Science*, 2004, **306**, 1301–1302.
- [34] H. Cölfen, M. Antonietti, *Mesocrystals and Nonclassical Crystallization*, John Wiley & Sons, Chichester, UK, 2008.
- [35] J. J. De Yoreo, P. U. P. A. Gilbert, N. A. J. M. Sommerdijk, R. L. Penn, S. Whitelam, D. Joester, H. Zhang, J. D. Rimer, A. Navrotsky, J. F. Banfield, A. F. Wallace, F. M. Michel, F. C. Meldrum, H. Cölfen, P. M. Dove, *Science*, 2015, **349**, article no. aaa6760.
- [36] M. A. Crenshaw, in *Skeletal Growth of Aquatic Organisms* (D. C. Rhoads, R. A. Lutz, eds.), Plenum Press, New York, 1980, 115–132.
- [37] C. Rollion-Bard, D. Blamart, J. P. Cuif, A. Juillet-Leclerc, *Coral Reefs*, 2003, **22**, 405–415.
- [38] K. Simkiss, *Am. Zool.*, 1984, **24**, 847–856.
- [39] E. Beniash, J. Aizenberg, L. Addadi, S. Weiner, *Proc. R. Soc. Lond. B*, 1997, **264**, 461–465.
- [40] L. Xiang, W. Kong, J. Su, J. Liang, G. Zhang, L. Xie, R. Zhang, *PLoS One*, 2014, **9**, article no. e113150.
- [41] L. Addadi, S. Raz, S. Weiner, *Adv. Mater.*, 2003, **15**, 959–970.
- [42] A. S. Mount, A. P. Wheeler, R. P. Paradkar, D. Snider, *Science*, 2004, **304**, 297–300.
- [43] A. V. Ivanina, H. I. Falfushynska, E. Beniash, H. Piontkivska, I. M. Sokolova, *J. Exp. Biol.*, 2017, **220**, 3209–3221.
- [44] H. Mutvei, “Biomineralization”, in *Int. Symp. on Problems of Biomineralization*, vol. 6, Schattauer Verlag, Stuttgart, New York, 1972, 96–100.
- [45] H. Mutvei, *Calcif. Tiss. Res.*, 1977, **24**, 11–18.
- [46] H. Mutvei, *Zool. Scr.*, 1978, **7**, 287–296.
- [47] H. Mutvei, in *Scanning Electron Microscopy II* (O. Johari, ed.), SEM Inc., Chicago Press, Chicago, 1979, 451–462.
- [48] B. Frérotte, A. Raguideau, J. P. Cuif, *C. R. Acad. Sci. Paris*, 1983, **297**, 383–388.
- [49] J. P. Cuif, Y. Dauphin, J. E. Sorauf, *Biominerals and Fossils through Time*, Cambridge University Press, Cambridge, UK, 2011, 490 pages.
- [50] Y. Dauphin, J. P. Cuif, J. Doucet, M. Salomé, J. Susini, C. T. Williams, *Mar. Biol.*, 2003, **142**, 299–304.

- [51] J. P. Cuif, O. Belhadj, S. Borensztajn, M. Geze, S. Trigoso-Santos, P. Prado, Y. Dauphin, *Heliyon*, 2020, **6**, article no. e04513.
- [52] J. D. Taylor, W. J. Kennedy, *Calcif. Tiss. Res.*, 1969, **3**, 274-283.
- [53] J. H. Waite, in *The Mollusca, Vol. 1, Metabolic Biochemistry and Molecular Biomechanics* (P. W. Hochachka, ed.), Academic Press, New York, 1983, 467-504.
- [54] E. M. Harper, *Palaeontology*, 1997, **40**, 71-97.
- [55] H. Nakahara, G. Bevelander, *Calcif. Tissue Res.*, 1971, **7**, 31-45.
- [56] M. Suzuki, S. Nakayama, H. Nagasawa, T. Kogure, *Micron*, 2013, **45**, 136-139.
- [57] J. P. Cuif, M. Burghammer, V. Chamard, Y. Dauphin, P. Godard, G. Le Moullac, G. Nehrke, A. Perez-Huerta, *Minerals*, 2014, **4**, 815-834.
- [58] J. P. Cuif, Y. Dauphin, G. Luquet, K. Medjoubi, A. Somogyi, A. Perez-Huerta, *Minerals*, 2018, **8**, article no. 370.
- [59] J. P. Cuif, Y. Dauphin, in *Biom mineralization, from Molecular and Nano-structural Analyses to Environmental Science* (K. Endo, T. Kogure, H. Nagasawa, eds.), Springer, Singapore, 2018, 349-357.
- [60] Y. Dauphin, *Palaont. Zeit*, 2001, **75**, 113-122.
- [61] J. P. Cuif, Y. Dauphin, P. Berthet, J. Jegoudez, *Geochem. Geophys. Geosys.*, 2004, **5**, 1-9.
- [62] M. Cusack, P. Chung, Y. Dauphin, A. Perez-Huerta, *Palaeontology*, 2010, **84**, 99-105.
- [63] Y. Dauphin, E. Dufour, *Micron*, 2008, **39**, 891-896.
- [64] Y. Dauphin, G. Luquet, A. Perez-Huerta, M. Salomé, *Connect. Tissue Res.*, 2018, **59**, 67-73.
- [65] J. Aizenberg, G. Lambert, L. Addadi, S. Weiner, *Adv. Mater.*, 1996, **8**, 222-226.
- [66] J. P. Cuif, Y. Dauphin, B. Farre, G. Nehrke, J. Nouet, M. Salomé, *Mineral. Mag.*, 2008, **72**, 233-237.
- [67] Q. Cheng, W. Hu, Z. Bai, *Front. Mar. Sci.*, 2021, **8**, article no. 657263.
- [68] M. Suzuki, H. Nagasawa, *Can. J. Zool.*, 2013, **91**, 349-399.
- [69] E. T. Degens, D. W. Spencer, *Comp. Biochem. Physiol.*, 1967, **25**, 553-579.
- [70] K. Simkiss, *Comp. Biochem. Physiol.*, 1965, **16**, 427-435.
- [71] M. A. Crenshaw, H. Ristedt, in *The Mechanisms of Mineralization in the Invertebrates and Plants* (N. Watabe, K. M. Wilbur, eds.), vol. 5, University of South Carolina Press, Columbia, 1976, 355-367.
- [72] F. Nudelman, B. A. Gotliv, L. Addadi, S. Weiner, *J. Struct. Biol.*, 2006, **153**, 176-187.
- [73] I. K. Kawakami, *Mem. Fac. Sci., Kyushu Univ.*, 1952a, **1**, 83-89.
- [74] I. K. Kawakami, *J. Fuji Pearl Institute*, 1952b, **2**, 1-4.
- [75] K. Wada, *Bull. Natl. Pearl Res. Lab.*, 1957, **3**, 167-174.
- [76] K. Wada, *Bull. Natl. Pearl Res. Lab.*, 1961, **36**, 703-828.
- [77] K. Wada, *Bull. Gemmol. Soc. Japan*, 1999, **20**, 47-62.
- [78] J. Taylor, E. Strack, "Pearl production", in *The Pearl Oyster* (P. C. Southgate, J. S. Lucas, eds.), Elsevier, Amsterdam, The Netherlands, 2008, 273-302.
- [79] J. P. Cuif, Y. Dauphin, L. Howard, J. Nouet, S. Rouzière, M. Salomé, *Aquat. Living Resour.*, 2011, **23**, 277-284.
- [80] A. Somogyi, K. Medjoubi, G. Baranton, V. Le Roux, M. Ribbens, F. Polack, P. Philippot, J. P. Samama, *J. Synchrotron Radiat.*, 2015, **22**, 1118-1129.
- [81] J. P. Cuif, Y. Dauphin, G. Luquet, O. Belhadj, S. Rouzière, M. Salomé, M. Cotte, A. Somogyi, K. Medjoubi, C. Lo, D. Saulnier, *Aquac. Res.*, 2019, **51**, 506-522.
- [82] Y. Dauphin, O. Belhadj, L. Bellot-Gurlet, M. Cotte, C. Lo, K. Medjoubi, A. Somogyi, M. Salomé, D. Saulnier, J. P. Cuif, *Mater. Charact.*, 2020, **163**, article no. 110276.
- [83] J. P. Cuif, A. Bendouan, Y. Dauphin, J. Nouet, F. Sirotti, *Anal. Bioanal. Chem.*, 2013, **405**, 8739-8748.
- [84] Y. Dauphin, E. Zolotoyabko, A. Berner, E. Lakin, C. Rollion-Bard, J. P. Cuif, P. Fratzi, *J. Struct. Biol.*, 2019, **205**, 121-132.
- [85] Y. Dauphin, *J. Biol. Chem.*, 2003, **278**, 15168-15177.
- [86] A. G. Checa, A. B. Rodriguez-Navarro, F. J. Esteban-Delgado, *Biomaterials*, 2005, **26**, 6404-6414.
- [87] B. Pokroy, J. P. Quintana, E. N. Caspi, A. Berner, E. Zolotoyabko, *Nat. Mater.*, 2004, **3**, 900-902.